Asian Journal of Chemistry; Vol. 27, No. 12 (2015), 4510-4516

ASIAN JOURNAL OF CHEMISTRY

http://dx.doi.org/10.14233/ajchem.2015.19206

Synthesis, Characterization and Toxicity Analysis of Some Mn(II), Co(II), Ni(II) and Cu(II) Complexes with N-*p*-Nitrobenzoyl-α-phenylalanine

C. ROSCA[1], V. SUNEL[2], M. CRETU[2], C. MITA[2], N. APOSTOLESCU[1], D. MARECI[1], C. MUNTEANU[3], I. RUSU[1], D. SIBIESCU[1], C. STAN[1] and D. SUTIMAN[1,*]

[1]Gheorghe Asachi Technical University of Iasi, Faculty of Chemical Engineering and Environmental Protection, 73 D. Mangeron Rd., Iasi 700050, Romania
[2]Alexandru Ioan Cuza University of Iasi, Faculty of Chemistry, B-dul Carol I, Nr. 11, RO-700506-Iasi, Romania
[3]Gheorghe Asachi Technical University of Iasi, Faculty of Mechanical Engineering, 73 D. Mangeron Rd., Iasi 700050, Romania

*Corresponding author: Fax: +40 232 271311; Tel: +40 232 27868; E-mail: sutiman@ch.tuiasi.ro

Received: 28 March 2015; *Accepted*: 15 June 2015; *Published online*: 29 August 2015; AJC-17499

The paper presents the synthesis and physico-chemical characterization of some Mn(II), Co(II), Ni(II) and Cu(II) complexes with N-*p*-nitrobenzoyl-α-phenylalanine and the determination of toxicity level (lethal dose). Elemental analysis, FTIR, UV-visible and XRD spectroscopy, electronic spin resonance (ESR), Mössbauer spectroscopy for the iron compound and the thermal stability with the FTIR analysis of the evolved gases were applied to characterize the metal complexes. All the compounds have an orthorhombic crystalline structure and have a thermal stability over 100 °C. The toxicity of the new compounds was tested on laboratory mice and was determined that Cu(II) compound has the lowest lethal dose compared with the pure ligand.

Keywords: N-(*p*-Nitrobenzoyl)-α-phenylalanine, Coordination compounds, Structure, Thermal analysis, Toxicity.

INTRODUCTION

Is well known the fact that some heterocyclic compounds have special applications in medicine due to their antidepressive[1], cardiotonic[2], antibacterial[3-5], antimycotic or antifungal[6-8] effects and new researches revealed analgesic and anti-inflammatory effects too[9-11]. N-Acylated amino acids are also known for their hepato-protector, antimicrobial, antitumoral effect[12-16]. Furthermore, these compounds are also good ligands for transition metals. In our work, we synthesized four complexes of Mn(II), Co(II), Ni(II) and Cu(II) with N-(*p*-nitrobenzoyl)-α-phenylalanine (NBFA). The organic ligand was synthesized at 10-12 ºC by condensation reaction of *p*-nitrobenzoic acid chloride with phenylalanine in a solution of sodium bicarbonate, the acid chloride being dissolved in anhydrous benzene. The product was purified by column chromatography on silica gel using as eluent a mixture of dichloromethane-methanol 9:2[17]. Ligand structure is shown in Fig. 1.

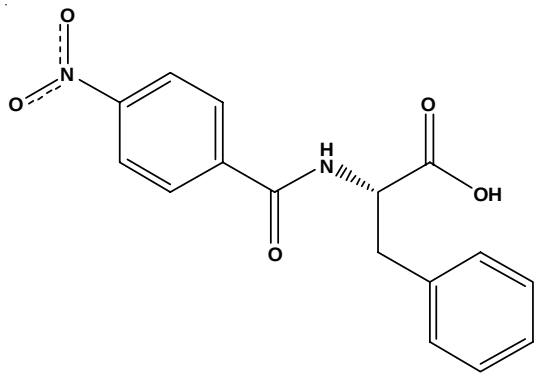

Fig. 1. Structure of N-(*p*-nitrobenzoyl)-L-phenylalanine (L)

EXPERIMENTAL

As reagents were used $MnCl_2 \cdot 4H_2O$ (> 99 %), $CoCl_2 \cdot 6H_2O$ (> 99 %), $NiCl_2 \cdot 6H_2O$ (> 99 %), $CuCl_2 \cdot 2H_2O$ (> 99 %), purchased from 'Sigma-Aldrich' Chem. Co and N-*p*-nitrobenzoil-α-phenylalanine (L) analytical grade. The complexes were prepared by addition of a 0.1 M ethanolic solution of N-(*p*-nitrobenzoyl)-L-fenylalanine (L) to the appropriate ethanolic solution of the metal halide in a 2:1 molar ratio. The initial mixtures were stirred for 1 h at 30 °C. The separation from the reaction medium was done by slow evaporation (few days) at 30 ºC, when the four complexes were obtained in solid state. The compounds were purified by successive recrystallizations in ethanol and finally were washed bidistilled water.

In order to determine the molar composition of these compounds the following investigations were carried out: elemental analysis of C, N, H by oxygen combustion and O by pyrolysis, on the Thermo Fisher Scientific equipment Flash EA-1112CHNS/O, the metal being calculated by difference. Data acquisition and interpretation was performed with specialized software - Eager 300. The FTIR spectra were obtained by means of a Perkin-Elmer Spectrum 100 apparatus, in the 4000-400 cm^{-1} range, in KBr pellets. The UV-visible absorption spectra of solid samples were performed with CAMSPEC 50 M single beam spectrophotometer provided with a diffuse reflectance sphere, using $BaSO_4$ pellets as blank, in the 190-1100 nm range. The number and energy of transition bands were resolved by the deconvolution of the original electronic diffuse reflectance spectra (DRS) using OrigineLab programs. The transitions assignation was performed using Tanabe-Sugano diagrams (for Mn(II), Co(II), Ni(II) and Cu(II)) and the molecular orbital diagram (for L)[18,19].

The electronic spin resonance spectra were performed using a CMS 8400 ESR equipment (3216.9 Gauss magnetic field corresponding to center of sample and 9030 MHz frequency) and was determined the spectroscopic scission factor g and the number of impair electrons belonging to each metallic atom, using diphenylpicrilhydrazine (DPPH) as standard. XRD analysis was performed by means of X'Pert PROMRD Panalytical Holland diffractometer and CuK_α radiation, determining the unit cell parameters and volume. In order to determine the changes which occur during the heating process we used a TG-EGA-FTIR apparatus consisting of a Diamond TG/DTA (Perkin Elmer) thermo-balance, a Spectrum 100 (Perkin Elmer) FTIR spectrophotometer, TG-FTIR (Perkin Elmer) gas transfer accessory (1.6 m stainless steel 1.5 mm tube heated at 220 °C) and a heated gas cell of 100 mm length with KBr windows (heated at 150 °C). The Spectrum TimeBase (Perkin Elmer) software records every 15 s a single spectrum within the 4000-700 cm^{-1}, at a resolution of 4 cm^{-1}. The analysis was run with the sample placed into a platinum crucible, under dynamic dry air atmosphere (100 mL min^{-1}) at a heating rate of 10 K min^{-1}, within the 35-700 °C temperature range.

The toxicity of the coordinative compounds was performed at the Central Laboratory for Drug Testing, "Grigore T. Popa" University of Medicine and Pharmacy, Iasi, on the mice (2 animals/group).

RESULTS AND DISCUSSION

Elemental analysis: The determined elemental composition corresponds, within the error limit of ± 0.35 %, to the following chemical formulae: $[M[(L)_2(H_2O)_2]$ where M = Mn, Co, Ni, Cu. The results are listed in Table-1. These were corroborated with the thermal analysis in order to determine the number of water molecules.

FTIR spectra: Key frequencies are listed in Table-2. Structural data of the ligand and the comparison of the complexes FTIR spectra allowed assigning the characteristic vibrations. High-frequency region contains bands determined by the stretching vibrations of: water molecule ν(O-H), NH group ν(N-H) and CH_2 ν(C-H). The wavenumbers of these bands correspond to the position expected from the structural data. In concerned range, the complexes spectra are complicated by the water bands. The characteristic bands with peaks at 3501, 3435, 3426, 3443 cm^{-1} are assigned to the ν(O-H) vibration. The lower intensity of ν(O-H) band for $[Cu[(L)_2(H_2O)_2]$ complex can be related with a difference between polarity of O-H bonds or one water molecule forms intermolecular hydrogen bond with oxygen atom of one C=O group. The CH_2 group frequencies are not sensitive at the metal cation presence.

TABLE-1
ELEMENTAL ANALYSIS DATA AND MOLECULAR FORMULA FOR $[M(L)_2(H_2O)_2]$

m.f.	Elemental analysis (%): Calcd. (Exp.)			
	C	H	N	M
$C_{32}H_{28}N_4O_{12}Mn$	53.31 (53.48)	3.52 (3.50)	7.44 (7.39)	7.27 (7.17)
$C_{32}H_{28}N_4O_{12}Co$	53.43 (53.48)	3.89 (3.79)	7.79 (7.77)	8.19 (8.28)
$C_{32}H_{28}N_4O_{12}Ni$	53.43 (53.44)	3.89 (3.95)	7.79 (7.70)	8.18 (8.21)
$C_{32}H_{28}N_4O_{12}Cu$	53.07 (53.12)	3.87 (3.81)	7.74 (7.77)	8.79 (8.83)

The values of stretching frequencies of N-H bond decrease in the following order (Table-2): L > Mn(II) > Co(II) ≥ Cu(II) > Ni(II). This process is accompanied by the decreasing of the bands intensity. Accordingly, the nitrogen atom of amide group is bonded to the metal cation.The ν(CO) frequencies of coordinated and the non-coordinated C=O groups are affected by the coordination of ligand to the metal by forming a trans-planar structure as well as by the intermolecular interactions.

The presence of the strong bands at 1646, 1643 and 1675 cm^{-1} is an indication of existence of neutral carboxyl group. The band at 1411 cm^{-1} is also assigned to symmetric stretching COO^- group frequency that partial overlaps with CH_2 bending frequency. By coordination the intensity of bending bands decreased by 400-300 cm^{-1} due to the lowering of the liberty degree of the vibration-rotation movement. The shift of frequency order indicates the increasing order of the M-O inter-action since the COO^- group becomes more asymmetrical. The change in the electronic density of the oxygen donor atom deter-mined the simultaneous shifting of the $\nu(COO^-)$ frequency bands. Difference between $\nu_{as}(COO)$ and $\nu_s(COO)$ values increases with the increasing of electronic density of metal cation and the ligand field effect, respectively (187, 190, 193 and 197 cm^{-1}) (Table-2).

The influence of metal cations on the amide II C=O group electronic density is almost the same, excepting the Cu(II) cation. This means that the ketonic bond becomes weaker and the amidic bond stronger. The fact is due to the displacement of the electron pair from the amidic nitrogen toward the metal determining the shortening of the N-H bond with the reorientation of the π electrons from the ketonic bond and the benzene ring (Fig. 2).

The formation of the M-O covalent bond lead both to the decrease of the C-O bond strength and the increase of C=O bond strength. The corresponding modifications appear in the variation of the two bonds stretching frequencies (Table-2).

UV-visible absorption spectra: Visible and near-IR spectra for solid ligand and complexes are shown in Fig. 3a and their deconvolution results are summarized in Table-3 and Fig. 3b.

TABLE-2
SHIFT OF CHARACTERISTIC VIBRATIONS IN THE FTIR SPECTRA OF THE SYNTHESIZED COMPOUNDS

Compound	ν(C=O) (amide I) (cm^{-1})	ν_{as}(COO) (cm^{-1})	ν(NH) (cm^{-1})	ν_{s}(COO) (cm^{-1})	ν(M–O) (cm^{-1})	ν(M–N) (cm^{-1})
Ligand	1730	1696	3174	1491	–	–
$Mn[L_2(H_2O)_2]$	1646	1598	3115	1411	563	609
$Co[L_2(H_2O)_2]$	1646	1601	3109	1411	531	620
$Ni[L_2(H_2O)_2]$	1643	1604	3086	1411	533	624
$Cu[L_2(H_2O)_2]$	1675	1609	3110	1412	520	657

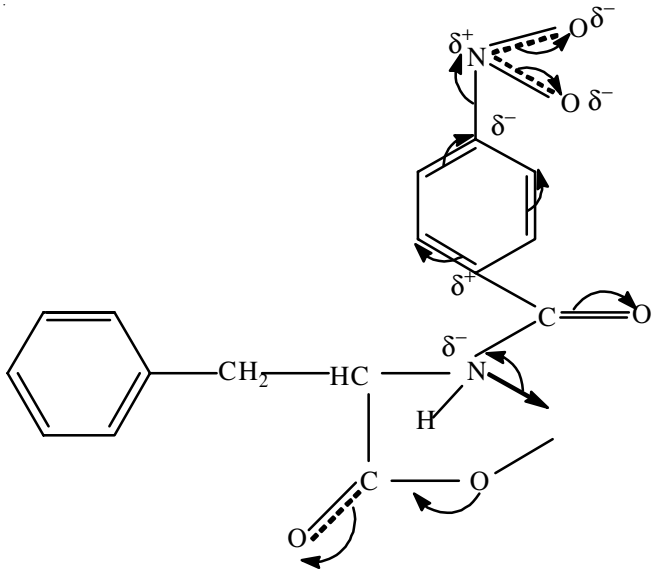

Fig. 2. Electronic effects on ligand determined in presence of metallic ion

TABLE-3
DR SPECTRAL DATA (λ, nm) FOR TRANSITIONS OF LIGAND AND COORDINATIVE COMPOUNDS

Compound	Ligand-ligand	Charge transfer	*d-d*
Ligand	242, 311, 375	–	–
$Mn[L_2(H_2O)_2]$	236, 347	–	438, 566
$Co[L_2(H_2O)_2]$	235, 343	450	582, 653, 705, 1150
$Ni[L_2(H_2O)_2]$	226, 316	–	471, 669, 777, 1072
$Cu[L_2(H_2O)_2]$	232, 324	445	686, 818, 998

All DR spectra of $M[L_2(H_2O)_2]$ coordinative compounds are typical for high spin complexes. Manganese(II) complex, $Mn[(L)_2(H_2O)_2]$, are very weakly coloured in yellow. The two week bands are due to Mn(II)–d^5 $^4T_{1g}(G)$-$^6A_{1g}$ (566 nm) and $^4T_{2g}(G)$-$^6A_{1g}$ (438 nm) forbidden transitions (Table-3). This pair of electronic transitions are generated by the distorted octahedral symmetry which suggests that the manganese(II) is coordinated by two ligand molecules on equatorial sites, and the two water molecules are on axial positions.

The complexity of the electronic spectrum of $[Co^{II}L_2]$ (Fig. 3a and Table-3) is a consequence of the tetrahedral distortion of square-planar symmetry of the cobalt (II) coordinative center due to the nonequivalent donor atoms of the ligand, steric hindrance and less to the Jahn-Teller effect. The $^4T_1(F)$–$^4A_2$ and $^4T_1(P)$–$^4A_2$ transitions of Co(II)-d^7 appear as multiple absorption in the near infrared and visible regions, respectively (Table-3). The intensity and the gap between these bands allow to made distinction between pseudo-square planar and tetrahedral symmetry of coordinative center. The relatively large bandwidths of deconvoluted original spectrum of $[Co^{II}L_2]$

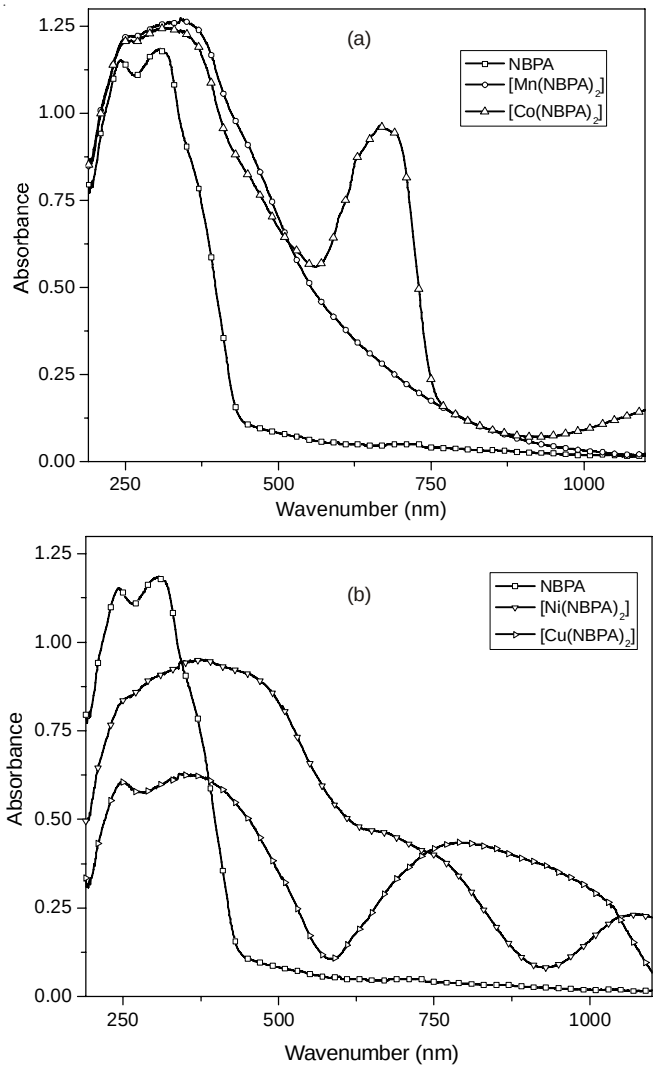

Fig. 3. Electronic DR spectra of ligand (L) and $[Mn(L)_2(H_2O)_2]$, $[Co(L)_2(H_2O)_2]$ (a), $[Ni(L)_2(H_2O)_2]$ and $Cu[(L)_2(H_2O)_2]$ complexes (b)

complex suggest that low symmetry field and vibrational structure may be responsible to the additional splitting of the ground state terms.

For visible and near-IR spectrum of $[Ni^{II}L_2]$ complex all three spin-allowed transitions, typical of d^8 high-spin complexes, were observed: $^3T_{2g}(F)$ - $^3A_{2g}$ (1072 nm), $^3T_{1g}(F)$-$^3A_{2g}$ (777 nm) and $^3T_{1g}(P)$ $^3A_{2g}$ (471 nm) (Table-3). In addition, a band corresponding to the spin-forbidden transition ^1E_g - $^3A_{2g}$ was observed at 669 nm, which is partially overlapped with the $^3T_{1g}(F)$ - $^3A_{2g}$ band (777 nm). Presumably, the higher energy states interact more with the larger and more polarizable N-donor atom than with the oxygen atom of L1 ligand which increases the effect of skeletal vibrations. This is equivalent with a vibronically induced electronic transition of all four

band transitions, three of them lying under a single broad envelope and a tetrahedral distorsion in the excitated states.[2]D ground state of Cu(II)–d^9 is spin and orbital deca-degenerated. Thus, all the electronic transitions are energy independent by the interelectronic repulsions. The electronic spectrum of solid [$Cu^{II}L_2$] (Fig. 3b and Table-3) shows three transition bands attributed to the tetrahedral distortion of the copper(II) symmetry center due to CuN_2O_2 chromofor plane and spin-orbital coupling coefficient of Cu(II), which is higher than 800 cm^{-1} [18]. Furthermore, the number and energy of *d-d* elec-tronic transitions of Cu(II) are influenced by the polarization of the Cu-N bonds. As consequence, the $^2T_{2g}$-^2E_g transition is splited in three bands in UV-near IR area (Table-3). The band centred at 445 nm was attributed to the Cu(d_{x2-y2})-NBPA(π^*) charge transfer transitions. The DR electronic spectrum of L_1 shows two intense bands due to n-π^* and π-π^* transitions in 200-400 nm range (Fig. 3a, Table-3). The n-π^* transition is split in two bands. Their wavelengths are determined by the the nitrogen and oxygen electronegativities and the electronic effect of the auxochromic groups: $\lambda_{n_N-\pi^*}$ = 374 nm and $\lambda_{n_O-\pi^*}$ = 311 nm. The band of π-π^* transition of phenyl rings is centered at 242 nm.

The coordination of ligand molecules to the metal cation led to the overlapping of n-π^* bands and hypsochromic shift of π-π^* transitions. From these, one could determine that the nitrogen forms with M(II) a bond with higher covalent degree than oxygen, according with Lewis basic hardness of donor-atoms. The hypsochromic shift of n_N-π^* transition increases with the increasing of Lewis compatibility between N-donor ligand and metal cation.

ESR spectroscopy: The spectrochemical scission factor (g) and the number of unpaired electrons for each central ion were calculated based on literature[20] according to the following relation:

$$N_x = N_e \frac{(I_x H^2_{max})_x}{(I_e H^2_{max})_c} \quad (1)$$

where: N_x and N_e represents the number of unpaired electrons of the studied sample and of the standard sample. N_e has the value 0.281×10^{20} impair electrons mL^{-1}. I_x and I_e are the signal amplitudes for the analyzed and respectively standard sample. $(H_{max})_x$ and $(H_{max})_e$ are the intensity values of the maximum magnetic field corresponding to the sample and to the standard.

The g factor is calculated according to the following relation:

$$g = g_e (H_x/H_e) \quad (2)$$

where g_e = 2.0055 for the standard sample. H_x and H_e represent the magnetic field corresponding to the centre of the studied sample spectrum and respectively of the standard H_e = 3216, 9 Gauss.

The above relations could be applied when both spectra curves (analyzed and standard), are of the same type (Gauss or Lorentz). For the complexes with organic ligands, the g value is higher than that of the free electron and is correlated with the arrangement of the ligands around the central atom. Table-4 presented the values for g factor, H_x and the number of unpaired electrons corresponding to each central atom. One may observe that all the complexes are paramagnetic and with high spin, M-L bond having a low covalent degree.

TABLE-4
VALUES OF ESR PARAMETERS FOR THE SYNTHESIZED COMPOUNDS

Compound	g	H_x	Number of unpaired electrons of the central ion
$Mn[L_2(H_2O)_2]$	2.0305	3257.00	4,89
$Co[L_2(H_2O)_2]$	2.0188	3229.90	2,91
$Ni[L_2(H_2O)_2]$	2.1770	3224.80	1.98
$Cu[L_2(H_2O)_2]$	2.0250	3193.50	0.96

XRD analysis: From the data obtained by the indexing of the synthesized complexes diffractograms results that they crystallize in the orthorhombic system, different from the tetragonal one of the ligand (Table-5).

The metallic ions are paramagnetic with high spin and achieve coordinative bonds by means of 4*s*, 4*p* and 4*d* orbitals in octahedral configuration sp^3d^2. From the values of unit cell parameters one can deduce that two organic ligands are in the xOy plane and the water molecules are in a perpendicular plane. The non-equivalence of water molecules from $Cu[L_2(H_2O)_2]$ is evidenced by the different crystallization system of this compound. Based on the above data we propose for the synthesized compounds the structures from Fig. 4.

Thermal analysis: Fig. 5 presented the TG curves for four complexes and the ligand.

The thermal decomposition parameters[21] are presented in Table-6. One can observe that the ligand melts at 165 ºC and decomposes in two stages, the first one starting just after the melting process. Due to the fact that the combustion temperature of the benzene is about 550 ºC we may suppose that in this stage are broken just the C-C and C-N bonds from the external chain of the benzene ring. In the second stage occurred the complete benzene ring/organic part oxidation up to carbon oxides.

TABLE-5
VALUES OF UNIT CELLS PARAMETERS

Parameters	Ligand	$Mn[L_2(H_2O)_2]$	$Co[L_2(H_2O)_2]$	$Ni[L_2(H_2O)_2]$	$Cu[L_2(H_2O)_2]$
a (Å)	14.3991	14.8797	15.2025	17.0309	7.1065
b (Å)	11.3057	10.4294	3.8527	3.0757	7.1065
c (Å)	4.1641	5.5277	13.6345	15.2390	15.3526
α (º)	90	90	90	90	90
β (º)	90	90	92.1020	92.2110	90
γ (º)	90	90	90	90	90
V $(Å)^3$	677.8826	857.8200	798.0400	767.6500	776.85
System	Orthorhombic	Orthorhombic	Monoclinic	Monoclinic	Tetragonal

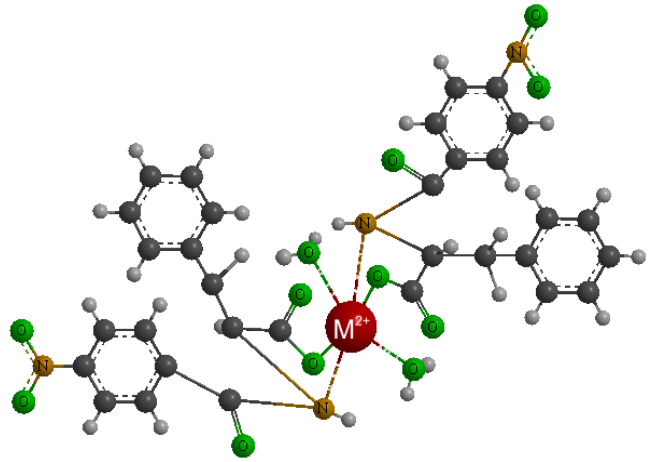

Fig. 4. Proposed structure for the synthesized complexes

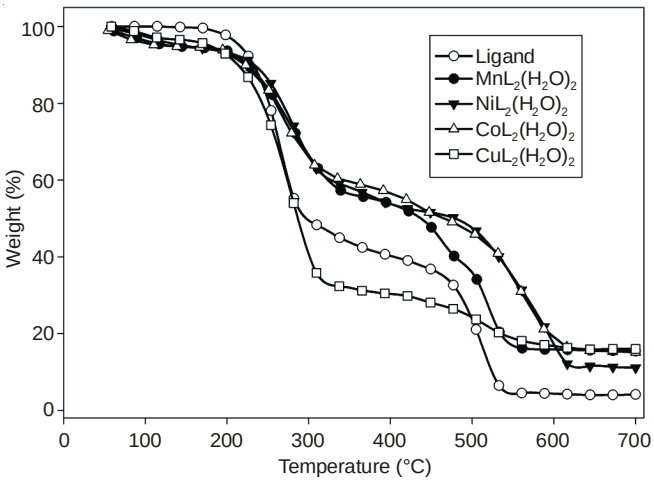

Fig. 5. TG curves of the samples measured in dry air at a flow rate of 100 mL min^{-1} (heating rate 10 K min^{-1}, initial mass: ligand = 5.291642 mg, $MnL_2(H_2O)_2$ = 4.992129 mg, $CoL_2(H_2O)_2$ = 5.205873 mg, $NiL_2(H_2O)_2$ = 5.092325 mg, $CuL_2(H_2O)_2$ = 4.887159 mg

The synthesized compounds decompose in four main steps. In the first stage (up to 180 ºC) occurs the lost of coordination water (about 6-7 %). It follows a main step (about 50 % weight loss) corresponding to the break between ketonic carbon and amidic nitrogen (Fig. 2) and the oxidation of organic radical.

The copper compound makes an exception due to the fact that the bond of the central ion with the nitrogen is much stronger and probably determines another mechanism of thermal decomposition. The activation energy of the main step respects the increase of the metal's electronegativity (according to Pauling[22]), *i.e.* of the M-N bond strength. The values of the residual mass are corresponding to the obtaining of metal oxides with maximum oxidation state.

The components of the gaseous mixtures released during the heating have been monitored and identified on basis of their FTIR reference gas spectrum available in the public spectrum library of NIST. FTIR spectra recorded the presence of H_2O, CO_2, CO[23], NH_3[24] and NO_2[25]. The evolution of the absorption at characteristic wavenumber for these gases with the temperature is presented in the Fig. 6.

According to the above analyses, it is observed that the decomposition products are similar both for ligand and the

TABLE-6
KINETIC PARAMETERS OF THE THERMAL DECOMPOSITION PROCESSES

	Temp. (°C)	Residual mass (%)	Effect/evolved compounds
Ligand	165 (Dec.)		endo
	165-406	39.9	exo/H_2O, CO_2, CO, NO_2
	406-800	4.40	exo/H_2O, NH_3, CO,CO_2, NO_2
	800-900	0.99	Exo, CO,CO_2,
	(157-405 ºC) E_a = 122 KJ/mol, n = 1.69, A = 1.44×10^{13} min^{-1}		
	(405-578 ºC) E_a = 195 KJ/mol, n = 1.11, A = 4.41×10^{12} min^{-1}		
$Mn[L_2(H_2O)_2]$	36-182	94.3	endo/H_2O
	182-374	55.2	exo/H_2O, CO_2, CO, NO_2
	374-479	39.8	exo/H_2O, CO_2, NH_3, NO_2
	479-590	11.8/9.9*	exo/H_2O, CO_2, NH_3, NO_2
	(182-374) E_a = 45.8 KJ/mol, n = 1.05, A = 1.16×10^7 min^{-1}		
$Co[L_2(H_2O)_2]$	36-159	94.7	endo/H_2O
	159-364	58.8	exo/H_2O, CO_2, CO, NO_2
	364-468	49.8	exo/H_2O, CO_2, CO, NO_2
	468-513	12.1/10.3*	exo/H_2O, CO_2, NH_3, CO
	(159-364) E_a = 52.2 KJ/mol, n = 0.77, A = $7.21 \cdot 10^{11}$ min^{-1}		
$Ni[L_2(H_2O)_2]$	62 -174	93.8	endo/H_2O
	178-354	56.1	exo/H_2O, CO_2, CO, NO_2
	448-644	11.1/10.4*	exo/H_2O, CO_2, NH_3, CO
	(178-354) E_a = 56.08 KJ/mol, n = 1.39, A = 1.93×10^{12} min^{-1}		
$Cu[L_2(H_2O)_2]$	67-155	92.6	endo/H_2O
	167-417	57.7	exo/H_2O, CO_2, CO, NO_2
	417-627	12.4/11.0*	exo/H_2O, CO_2, NH_3, CO
	(167-417) E_a = 57.4 KJ/mol, n = 0.54, A = 3.03×10^7 min^{-1}		

*Practical/theoretical-calculated as metal oxide

metal complexes. We have to mention that the gas products are in agreement with the results presented in literature for similar compounds[26-30].

According to the electronic structure, presented in Fig. 6, results that due to the attracting–I effect of the NO_2^- group occurs a displacement of the π electrons, which are more mobile toward this group that is partially positively charged on the carbon atom (C-N), determining a weakening of the N–M(II) bond and easier breaking of NO_2 group. Thus, it becomes the weakest bond from the system and is the first one that breaks at heating. On the other hand, p-π conjugation of the electrons from the double bond C=O of carboxyl groups and, accordingly, the displacement of electron pairs of oxygen to the carbon atom, strengthens the covalent O-M bond. A further proof of the proposed structure [coordination at nitrogen atom and covalent bond at the oxygen atom (Fig. 6)] is the presence of NH_3 in the decomposition gases at temperatures above 400 °C. Ammonia can be formed from the NH radical remained after the breaking from metal, without further oxidation which normally occur at temperatures above 900 ºC and only in the presence Pt catalysts.

The evolved gases analysis confirms our previous supposition *i.e.* NO_2 appears in the main step of the decomposition and ammonia results only at higher temperatures.

It is concluded that the general decomposition process is:

$$M[L_2(H_2O)_2]_{(s)} \xrightarrow{t°C} MO_{(s)} + B_{(g)} + 2H_2O_{(g)}$$

where B: H_2O, CO_2, CO, NO_2, NH_3.

Toxicity analysis: The acute toxicity resides in the mortality evaluation produced by the contact substance by any

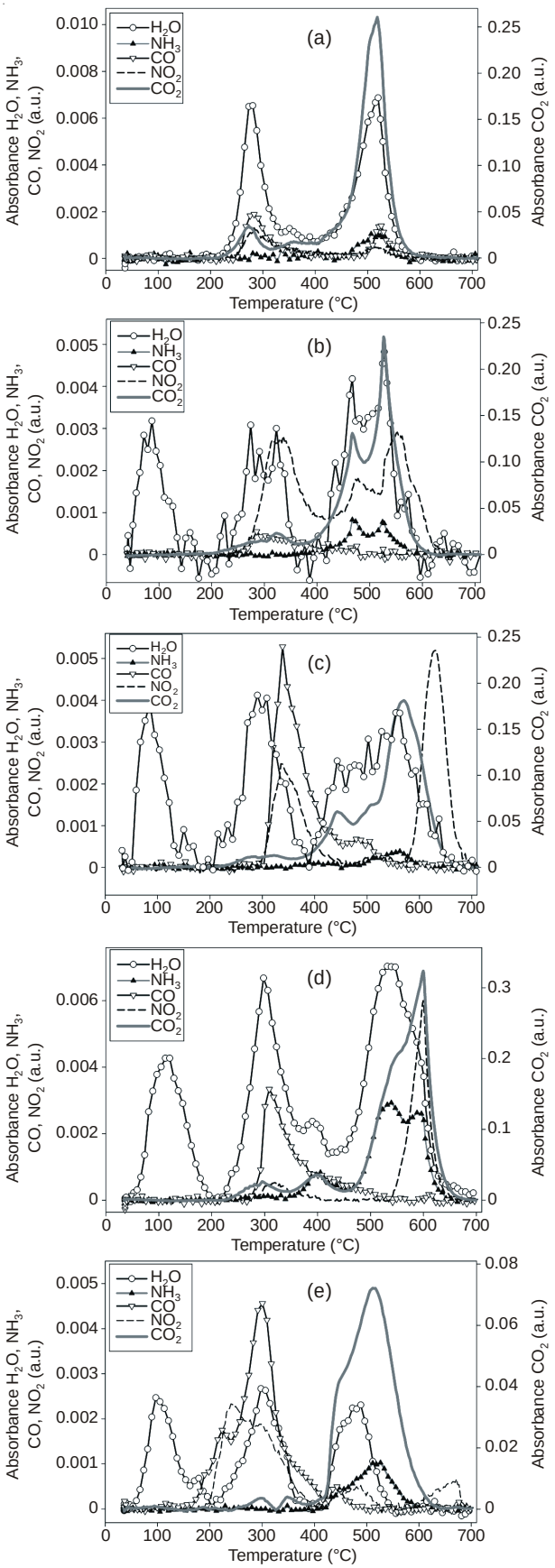

Fig. 6. IR absorbance *vs.* temperature curves of identified evolved gaseous species from samples in air, measured in air by online-coupled TG-FTIR system (heating rate 10 K min^{-1}; air flow rate 100 mL min^{-1}). (a) ligand, (b) $Mn[L_2(H_2O)_2]$, (c) $Co[L_2(H_2O)_2]$, (d) $Ni[L_2(H_2O)_2]$, (e) $Cu[L_2(H_2O)_2]$

kind of administration. The best indication in interpreting the results is given by the dose that kills 50 % of the experimental animals (LD_{50}), test that became indispensable for the new substances characterization[31]. Due to the fact that the three compounds could have antitumoral action, acting as anti-metabolites, it was performed the gradual testing of toxicity, determining LD_{50}. Mice are the most sensitive animals for the toxicity determination and we used sets of ten animals of 20 ± 2 g, of both sexes with a security limit of 30 %. The insoluble in water products were suspended in Twen 80 and injected intraperitoneal on a daily basis. The mice were monitored for 7 days, determining LD_{50} according to the Spearman-Karber method[32]. The obtained results are listed in Table-7.

TABLE-7
TOXICITY DETERMINATION OF STUDIED COMPOUNDS

Compound	LD_{50} (mg/kg body)
Ligand	6014
$Mn[L_2(H_2O)_2]$	5820
$Co[L_2(H_2O)_2]$	5890
$Ni[L_2(H_2O)_2]$	5848
$Cu[L_2(H_2O)_2]$	5766

As can be seen from the above data, all compounds present low toxicity similar to that of the ligand. Among these the highest toxic potential is presented by $[Cu(L)_2(H_2O)_2]$. The result is normal if we take into account the literature according to which the use of N-acyl-aminoacids in different combinations positively influence the toxicity degree[14,17,18,33,34].

Conclusion

We have synthesized four new compounds of N-*p*-nitrobenzoyl-α-phenylalanine with Mn(II), Co(II), Ni(II) and Cu(II), which were characterized by physico-chemical methods in order to determine their structures and properties. All compounds are crystalline (orthorhombic, monoclinic and tetragonal) with the ligands positioned in horizontal plane and the water molecules in vertical plane. The thermal stability is in direct concordance with the ionic radii and the electro-negativity, the decomposition mechanism being the classic one. The compounds' toxicity is similar to the ligand making them useful in different domains (medicine, cosmetics manufacture or religious artifacts corrosion inhibitors[35-38]).

REFERENCES

1. F. Clerici, D. Pocar, M. Guido, A. Loche, V. Perlini and M. Brufani, *J. Med. Chem.*, **44**, 931 (2001).
2. T. Onkol, B. Çakir and M.F. Sahin, *J. Chem.*, **28**, 461 (2004).
3. A. Varvarason, A. Tantili-Kakoulidou, T. Siatra-Papastasikoudi and E. Tiligada, *Arzneimittelforschung*, **50**, 48 (2000).
4. M. Gökce, B. Çakir, K. Erol and M.F. Sahin, *Arch. Pharm.*, **334**, 279 (2001).
5. O. Pintilie, L. Profire, V. Sunel, M. Popa and A. Pui, *Molecules*, **12**, 103 (2007).
6. K. Zamani, K. Faghifi, I. Tefighi and M.R. Sharlatzadeh, *Turk. J. Chem.*, **28**, 95 (2004).
7. X.J. ZouL.H. LaiG.Y. JinZ.X. Zhang. X.-J. Zou, L.-H. Lai, G.-Y. Jin and Z.-X. Zhang, *J. Agric. Food Chem.*, **50**, 3757 (2002).
8. H. Chen, Z. Li and Y. Han, *J. Agric. Food Chem.*, **48**, 5312 (2000).
9. S. Schenone, O. Bruno, A. Ranise, F. Bondavalli, W. Filippelli, G. Falcone, L. Giordano and M.R. Vitelli, *Bioorg. Med. Chem.*, **9**, 2149 (2001).

10. L. Labanauskas, V. Kalcas, E. Uderenaite, P. Gaidelis, A. Brukstus and V. Dauksas, *Pharmazie*, **56**, 617 (2001).
11. E. Palaska, G. Sahin, P. Kelicen, N.T. Durlu and G. Altinok, *Farmaco*, **57**, 101 (2002).
12. V. Sunel, C. Lionte, M. Popa, O. Pintilie, P. Mungiu and S. Teleman, *Eur. Chem. Tech. J.*, **4**, 201 (2002).
13. O. Pintilie, V. Sunel, L. Profire and A. Pui, *Farmacia*, **55**, 345 (2007).
14. M. Moise, V. Sunel, L. Profire, M. Popa and C. Lionte, *Farmacia*, **56**, 283 (2008).
15. V. Sunel, C. Lionte, C. Basu and C. Cheptea, *Chem. Indian J.*, **2**, 1 (2005).
16. V. Sunel, M. Popa, J. Desbrières, L. Profire, P. Otilia and L. Catalina, *Molecules*, **13**, 177 (2008).
17. M. Yadav, D. Behera and U. Sharma, *Corros. Eng. Sci. Technol.*, **48**, 19 (2013).
18. M. Moise, V. Sunel, L. Profire, M. Popa, J. Desbrieres and C. Peptu, *Molecules*, **14**, 2621 (2009).
19. A.B.P. Lever, Inorganic Electronic Spectroscopy, Elsevier, New York, edn 2, p. 712 (1984).
20. D.S. Bohle, A. Zafar, P.A. Goodson and D.A. Jaeger, *Inorg. Chem.*, **39**, 712 (2000).
21. N.S. Bhave and R.B. Kharat, *J. Inorg. Nucl. Chem.*, **43**, 414 (1981).
22. N.A. Liu and W.C. Fan, *Thermochim. Acta*, **338**, 85 (1999).
23. L. Pauling, General Chemistry, Scientific Ed., Bucharest, p. 183 (1972).
24. N.I.S.T. Chemistry Webbook Standard Reference Database No, 69, June 2005 Release (http://webbook.nist.gov/chemistry).
25. J. Madarász, I.M. Szilágyi, F. Hange and G. Pokol, *J. Anal. Appl. Pyrolysis*, **72**, 197 (2004).
26. J. Madarász, P.P. Varga and G. Pokol, *J. Anal. Appl. Pyrolysis*, **79**, 475 (2007).
27. O. Shulga and J. Dunn, *Thermochim. Acta*, **410**, 15 (2004).
28. L. Jie, L. Yuwen, S. Jingyan, W. Zhiyong, H. Ling, Y. Xi and W. Cunxin, *Thermochim. Acta*, **467**, 20 (2008).
29. N. Sasidharan, B. Hariharanath and A.G. Rajendran, *Thermochim. Acta*, **520**, 139 (2011).
30. S. Materazzi, S. Aquili, C. Bianchetti, G. D'Ascenzo, K.M. Kadish and J.L. Bear, *Thermochim. Acta*, **409**, 145 (2004).
31. S. Materazzi, S. Aquili, K. Kurdziel and S. Vecchio, *Thermochim. Acta*, **457**, 7 (2007).
32. E. Dommer, Animal Experiments in Pharmacological Analysis, Charles C. Thomas, Springfield, p. 283 (1971).
33. M.A. Hamilton, R.C. Russo and R.V. Thurston, *Environ. Sci. Technol.*, **12**, 417 (1978).
34. G.L. Gravatt, B.C. Baguley, W.R. Wilson and W.A. Denny, *J. Med. Chem.*, **37**, 4338 (1994).
35. N.M.A. El-Salam, N.S. Mostafa, G.A. Ahmed and O.Y. Alothman, *Wulfenia*, **3**, 303 (2013).
36. D. Mareci, R. Chelariu, I. Rusu, N. Melniciuc-Puica and D. Sutiman, *Eur. J. Sci. Theol.*, **6**, 57 (2010).
37. D. Mareci, R. Chelariu, D. Sutiman and I. Rusu, *Eur. J. Sci. Theol.*, **7**, 121 (2011).
38. D. Sutiman, I. Rusu, R. Chelariu, G. Lisa, V. Diaconescu and D. Mareci, *Eur. J. Sci. Theol.*, **8**, 215 (2012).